

## RESEARCH ARTICLE

Editorial Process: Submission:09/29/2023 Acceptance:03/02/2024

# Dynamic Contrast Enhanced-MRI and Apparent Diffusion Coefficient Quantitation for Differentiate Hepatocellular Carcinoma from Hepatocellular Adenoma

Hayder Suhail Najm Alareer<sup>1</sup>, Hayder Jasim Taher<sup>2</sup>, Ayoob Dinar Abdullah<sup>3\*</sup>

## Abstract

**Background:** Due to their overlapping radiological characteristics, hepatic lesions, such as hepatocellular carcinoma (HCC) and hepatocellular adenoma (HCA), present a substantial diagnostic challenge. Accurate differentiation between HCC and HCA is essential for the best clinical treatment and therapeutic decision-making. This study aims to assess the potential role of DCE-MRI and Apparent Diffusion Coefficient (ADC) quantitation in the diagnosis of hepatocellular carcinoma (HCC) from hepatocellular adenoma (HCA). **Methods:** 103 patients (56 HCC, 47 HCA) with histopathologically proven hepatocellular lesions were the subjects of a cross-sectional investigation. A standardized imaging technique was used for DCE-MRI on all patients. Diffusion-weighted imaging (DWI) provided the ADC values. The diagnostic efficacy of DCE-MRI and ADC in differentiation was evaluated using statistical analyses, such as t-tests and receiver operating characteristic (ROC) curve analysis. SPSS VER 16 was used for the analysis of the collected data. **Results:** A total of 103 patients (female: male= 52:51, 57.14±3.09 years) were included in the study. The study revealed significant differences in DCE-MRI parameters and ADC values between HCC and HCA lesions. ADC value was significantly lower in HCC than in HCA ( $p < 0.001$ ). The area under the curve (AUC) was 0.78 (95% CI: 0.69-0.87) for ADC, 0.84 (95% CI: 0.76-0.91) for  $K_{trans}$ , and 0.72 (95% CI: 0.62-0.82) for  $V_e$ . Sensitivity and specificity for ADC were 76.59% and 71.42%, respectively. Also, PPV and NPV of ADC were 69.23% and 78.43%, respectively. Sensitivity and specificity for  $K_{trans}$  were 82.14% and 76.59%, respectively. Also, PPV and NPV of  $K_{trans}$  were 80.7% and 78.26%, respectively. **Conclusion:** In conclusion, DCE-MRI-derived parameters, along with ADC values, exhibit promise as non-invasive tools for differentiating HCC from HCA.

**Keywords:** DCE-MRI- apparent diffusion coefficient- hepatocellular carcinoma- hepatocellular adenoma

*Asian Pac J Cancer Prev*, 25 (3), 931-937

## Introduction

Hepatocellular carcinoma (HCC) and hepatocellular adenoma (HCA) are two different liver cancers that pose substantial difficulties in proper diagnosis and therapy due to their overlapping radiological and histological characteristics [1]. It is essential to distinguish between these entities since they have unique clinical behaviors and therapeutic approaches. Interobserver variability and sampling mistakes may limit conventional diagnostic techniques like histopathological investigation [2]. HCC is still the fourth most common cancer-related cause of death worldwide. Developing new efficient methods is important because clinical diagnosis and treatment options are still somewhat limited [3].

Using cutting-edge imaging techniques, quantitative imaging analysis involves objectively evaluating tumor properties, such as size, shape, texture, and enhancing

patterns. In this setting, imaging techniques, including positron emission tomography (PET), contrast-enhanced computed tomography (CT), and magnetic resonance imaging (MRI), have become more popular [4]. These methods can offer essential insights into the pathophysiological variations between HCC and HCA using quantitative parameters, including tumor density, perfusion, and metabolic activity [5].

Dynamic contrast-enhanced (DCE) imaging involves the acquisition of serial images during the passage of a contrast agent through the vascular system and tissues [6].  $K_{trans}$  (transfer constant),  $K_{ep}$  (rate constant), and  $V_e$  (extravascular extracellular volume fraction) are three of the derived parameters that show promise as quantitative metrics for revealing tumor vascularization, perfusion, and permeability. Recent studies have focused on these variables because they provide insightful data beyond traditional morphological assessments [7].

<sup>1</sup> Department of Radiology, College of Health and Medical Technology, Al-Ayen University, Thi-Qar, Iraq. <sup>2</sup>Department of Radiology, Hilla University College, Babylon, Iraq. <sup>3</sup>Radiology Department, Al-Manara college for medical science, Maysan, Iraq. \*For Correspondence: ayoobdinara81@gmail.com

$K_{trans}$ , the rate of contrast agent transfer between the blood plasma and the extravascular extracellular space, reflects tissue perfusion and capillary permeability [8].  $K_{ep}$ , the efflux rate constant from the extravascular extracellular space, provides insights into the vascular exchange and leakage [9].  $V_e$  is a representation of the tumor tissue's fractional extracellular volume. DCE imaging provides a functional perspective that can help characterize the underlying pathophysiology of liver lesions by examining these characteristics [10].

The effectiveness of  $K_{trans}$ ,  $K_{ep}$ , and  $V_e$  in distinguishing HCC from HCA has been investigated in several studies. A study by Bane et al. [11] showed that  $K_{trans}$  values were significantly higher in HCC compared to HCA, demonstrating the more aggressive angiogenic nature of HCC. In a different study by Lewin et al. [12], it was found that HCC had raised  $K_{ep}$  values, which indicated enhanced vascular permeability, while HCA had higher  $V_e$  due to more sinusoidal gaps. These results imply that these variables might be biomarkers to differentiate between the two entities.

The ADC reflects the mobility of water molecules within tissues, which is produced from diffusion-weighted imaging (DWI). Different cellular designs and densities between HCC and HCA lead to different water diffusion properties [13]. HCC often displays lower ADC values due to its increased cellular density and constrained water diffusion than the somewhat less cellular and more diffusely structured HCA. ADC results can be quantitatively analyzed to produce data that can be used to differentiate between various lesions [13].

The present study aims to evaluate the potential role of DCE-MRI and ADC quantitation in diagnosing hepatocellular liver tumors. A thorough comprehension of the quantitative insights offered by  $K_{trans}$ ,  $K_{ep}$ , and  $V_e$  may improve the precision of diagnosis and guide treatment choices, resulting in better outcomes for patients with HCC and HCA.

## Materials and Methods

### Study Design and Patients Selection

This prospective cross-sectional study aimed to assess the utility of DCE-MRI and ADC quantitation for differentiating HCC from HCA. Ethical approval was obtained from Tehran University of Medical Sciences, International Campus (TUMS-IC), code (IR.TUMS.SPH.REC.1398.227). We identified 103 patients with hepatocellular liver tumors (51 men and 52 women, ages 18 to 86) referred to our institution for response assessment after receiving ethical approval from the Tehran University of Medical Sciences, International Campus (TUMS-IC). These patients were assessed by conventional MRI with DCE perfusion and compared with histopatholograms.

**Study Population:** The study was carried out in the Medical Imaging Center of the Imam Khomeini Hospital. Inclusion criteria encompassed patients with histopathologically confirmed HCC or HCA, pre-treatment DCE-MRI, diffusion-weighted imaging (DWI) data availability, and no prior treatment interventions. Patients with contraindications to MRI or gadolinium-based

contrast agents were excluded.

### Imaging Protocol

MRI scans were done on patients using a Philips Ingenia 1.5 Tesla MRI scanner (Philips Medical System, Amsterdam, the Netherlands) with a dedicated phased-array abdominal coil.

T1-weighted, T1 in and out phase, T2-weighted, and heavy T2 pulse sequences were used to examine the images by the differences in the signal strength, site, shape, size, and relationship of the lesions to the surrounding structures at the noncontract. The dynamic pictures from our Gd-DTPA MRI research were then evaluated to look for any differences in the enhancement pattern of the lesions with an accurate localization. We examined the diffusion-weighted imaging (DWI) research with the b-value (50,400,800) to assess the additional diagnostic value in identifying and characterizing the hepatic focal lesions. When a lesion showed higher signals to the healthy liver parenchyma on high-b-value images and when the ADC (apparent diffusion coefficient) map revealed a value lower than or equal to the liver parenchyma, restricted diffusion was considered. Readers assessed the ADC map qualitatively by contrasting it with the parenchyma of the normal surrounding liver. The T2 shine-through effect, observed in hemangiomas and cysts, is thought to be the bright signal on both diffusion pictures and ADC maps.

A single observer (H.J.T., with five years of abdominal imaging experience) blinded to the clinical history, imaging reports, and pathologic outcomes evaluated the ADC values for each lesion. On the MR console, ADC maps were obtained using post-processing software. The regions of interest (ROIs) were placed on the ADC maps and meticulously drawn by hand to contain the whole lesions without necrotic cores if present. The locations of lesions that were difficult to spot on DWI were found using T2-weighted and/or contrast-enhanced T1-weighted images. To prevent intrahepatic vessels and motion artifacts, the ROIs in the surrounding organ. The average, minimum, maximum, and standard deviation values of each ADC were determined based on three measurements.

### Data analysis

All patients' MRI images were evaluated and analyzed by a committee of highly experienced radiologists in a medical imaging center, who were blind to abnormal outcomes. Members of our institution's pathology department evaluated histopathology.

The statistical data were analyzed using SPSS, t-tests, and chi-square. P-values of 0.05 or below were considered significant for all outcomes. Diagnostic indices for MR imaging techniques were calculated based on sensitivity, specificity, positive and negative predictive values, and positive and negative probability ratios.

### Diagnostic Indices Calculation

#### Sensitivity

Defined as the proportion of true positive cases (correctly identified HCC) among all individuals with HCC. It is calculated using the formula:

$$\text{Sensitivity} = \frac{\text{True Positives}}{\text{True Positives} + \text{False Negatives}} \times 100\%$$

### Specificity

Indicates the proportion of true negative cases (correctly identified HCA) among all individuals with HCA. It is calculated as follows:

$$\text{Specificity} = \frac{\text{True Negatives}}{\text{True Negatives} + \text{False Positives}} \times 100\%$$

### Positive Predictive Value (PPV)

Represents the probability that a patient with a positive test result truly has HCC. It is calculated using the formula:

$$\text{PPV} = \frac{\text{True Positives}}{\text{True Positives} + \text{False Positives}} \times 100\%$$

### Negative Predictive Value (NPV)

Indicates the probability that a patient with a negative test result truly does not have HCC. Calculated as:

$$\text{NPV} = \frac{\text{True Negatives}}{\text{True Negatives} + \text{False Negatives}} \times 100\%$$

## Results

A total of 103 patients (Female: male= 52:51, 56.17±3.09 years) were included in the study (Table 1). Table 2 reports the mean and standard deviation for the values of each MRI parameter in both HCC and HCA groups. According to the reported results based on analysis with the Mann-Whitney test, the difference in the values of each of the MRI parameters (ADC,  $K_{trans}$ ,  $K_{ep}$ ,  $V_e$ ) between the HCC and HCA groups is significant, and the p-value for each of these parameters is less than 0.001. (Figure 1) (p<0.001).

Based on the analyses, the diagnostic value of each

Table 1. Demographic and Clinical Feature of the Studied Population

Population feature	
Gender N(%)	
Male	51(49.5)
Female	52(50.5)
Age (Mean ± SD)	56.17±3.09
Lesion number (Mean ± SD)	1.95±1.27
Lesion size in mm (Mean ± SD)	15.74±8.17

Table 2. The Difference between MRI Parameters (ADC,  $K_{trans}$ ,  $K_{ep}$ , and  $V_e$ ) for HCC and HCA Lesions

		N	Mean±SD	P-value
ADC-mean	HCC	56	1.23±0.36	<0.001
	HCA	47	1.67±0.43	
$K_{trans}$	HCC	56	0.90±0.21	<0.001
	HCA	47	0.60±0.19	
$K_{ep}$	HCC	56	2.44±1.01	<0.001
	HCA	47	1.63±0.92	
$V_e$	HCC	56	0.22±0.18	<0.001
	HCA	47	0.34±0.19	

MRI parameter alone for differentiating HCC from HCA is reported for ADC,  $K_{trans}$ ,  $K_{ep}$ , and  $V_e$  parameters. ROC curves for MRI parameters are shown in Figure 2, Figure 3, and Figure 4. The true positive rate (also known as sensitivity) is plotted on the y-axis of the ROC curve above. At the same time, the false positive rate (also known as 1 - specificity) is plotted on the x-axis. The proportion of true positives that are accurately detected is measured by sensitivity, whereas the proportion of actual negatives is measured by specificity.

The AUC and optimal cut-off and the relevant sensitivity, specificity, positive predictive value (PPV) and negative predictive value (NPV), and positive and

Table 3. The Optimal Diagnostic Performance of ADC,  $K_{trans}$ ,  $K_{ep}$ , and  $V_e$  to Differentiate HCA and HCC Lesions based on ROC Curve Analysis

	Sensitivity	Specificity	AUC	PPV	NPV	Optimal Cut-off
ADC	76.59%	71.42%	0.78 (95% CI: 0.69-0.87)	69.23%	78.43%	1.44
$K_{trans}^1$	82.14%	76.59%	0.84 (95% CI: 0.76-0.91)	80.70%	78.26%	0.746
$K_{ep}^2$	83.92%	51.06%	0.71 (95% CI: 0.62-0.81)	67.14%	72.72%	1.529
$V_e^3$	74.46%	69.64%	0.72 (95% CI: 0.62-0.82)	67.30%	76.47%	0.251

<sup>1</sup>forward volume transfer constant; <sup>2</sup>reverse volume transfer constant; <sup>3</sup>extravascular extracellular space volume fraction

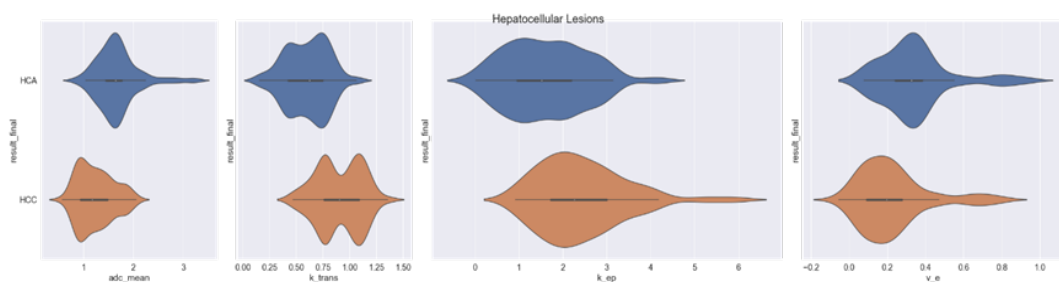


Figure 1. The Amount of MRI Parameters (ADC,  $K_{trans}$ ,  $K_{ep}$ , and  $V_e$ ) in HCC and HCA Lesions

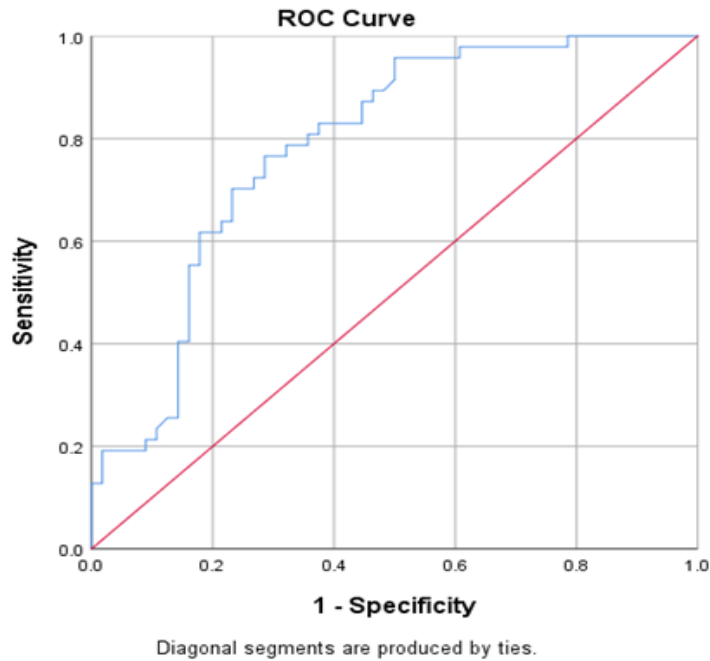


Figure 2. The ROC Curve of ADC Values for Differentiating HCC and HCA Lesions.

negative likelihood ratios for all MRI parameters ( $V_e$ ,  $K_{ep}$ ,  $DCE K_{trans}$ ) are extracted from ROC curve (Figure 2,3). The sensitivity, specificity, PPV, and NPV in the best

cut-off for each parameter are reported in Table 3. Also, the true positives, true negative, false positive, and false negative for the cut-off is reported in Table 4.

Table 4. The Result of Diagnosis based on an Optimal Cut-off of ADC,  $K_{trans}$ ,  $K_{ep}$ , and  $V_e$  to Differentiate HCA and HCC Lesions

	True Positive	True Negative	False Positive	False Negative
ADC	36	40	16	11
$K_{trans}$	46	36	11	10
$K_{ep}$	47	24	23	9
$V_e$	35	39	17	12

### Discussion

Due to their similar radiological characteristics, the differentiation between HCC and HCA remains a diagnostic challenge. In the present study, we evaluated the role of DCE-MRI and ADC as non-invasive methods for differentiating between these entities.

Our study showed that the pharmacokinetic parameters obtained from DCE-MRI differed noticeably between HCC and HCA. In comparison to HCA, the  $K_{trans}$  values

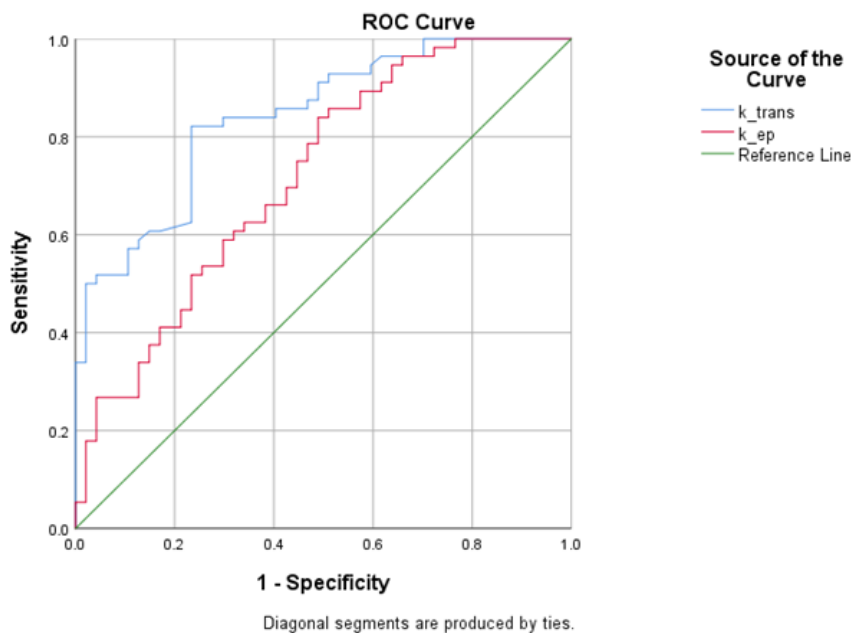


Figure 3. The ROC Curve of  $K_{trans}$  and  $K_{ep}$  Values for Differentiating HCC and HCA Lesions.

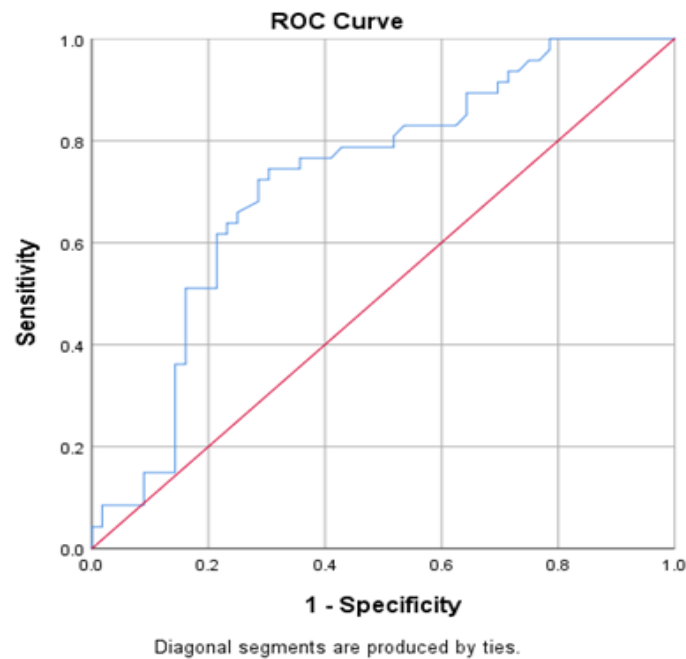


Figure 4. The ROC Curve of  $V_e$  Values for Differentiating HCC and HCA Lesions

in HCC were substantially higher. This finding aligns with earlier studies that highlight the aggressive angiogenic character of HCC, which leads to elevated contrast agent uptake and enhanced microvascular permeability [14]. As a result of its less aggressive vascularization and the presence of sinusoidal spaces, HCA displayed lower  $K_{trans}$  values in contrast. These results are consistent with studies that have shown the value of DCE-MRI in classifying liver lesions according to their vascular characteristics [15, 16].

It has been shown that changes in ADC values occur soon after treatment and strongly correspond with tumor necrosis [17]. Additionally, MRI is chosen over all other imaging techniques for detecting HCA tumors and their subtypes. According to recommendations, a dynamic MRI or CT scan should be performed once an ultrasound reveals a nodule in a patient's liver [18]. However, several clinical guidelines for identifying HCC currently specify DCE-MRI as the first-line imaging technique due to its excellent diagnostic accuracy [18]. The study conducted by Abdullah et al. (2024) showed that employing texture analysis on ADC MR images offers a feasible and objective methodology for discerning HCA from HCC in the liver [19]. According to Lee et al., study DWI using an ADC map is a quantitative imaging technique that is not significantly impacted by changes in gain factors. Additionally, several parameters obtained from ADC revealed significant differences between benign and malignant soft-tissue tumors [20].

Our analysis of the ADC values further enhanced the differentiation between HCC and HCA. When compared to HCA, the ADC values were much lower in HCC. The variation in cellular density and tissue architecture between the two lesions is responsible for this variance. Due to its high cellularity level, HCC exhibited restricted water diffusion and subsequently lower ADC values [21]. In contrast, the less cellular nature of HCA allows for

more unrestricted diffusion and larger ADC values. These ADC results support the ability of DWI to identify the features of hepatic lesions [18].  $K_{trans}$  values were observed to be considerably greater in HCC lesions compared to HCA lesions in the study by Taouli et al. [22], indicating enhanced microvascular permeability and angiogenesis in HCC. Additionally, HCC had higher  $K_{ep}$  values than normal, indicating more contrast agent extravasation. Due to the increasing number of sinusoidal spaces in HCA,  $V_e$  values were discovered to be higher. These results showed the ability of DCE-MRI-derived parameters to distinguish between these hepatic lesions. In line with increased tumor vascularity and permeability, the findings of the Ichikawa et al. [23] study showed that  $K_{trans}$  values were considerably higher in HCC than in HCA.  $V_e$  values were discovered to be lower in HCC, reflecting the lesions' more cellular and compact character.  $K_{trans}$  values were found to be significantly higher in HCC lesions compared to HCA lesions, according to Kwon et al. [24], indicating enhanced neovascularization and angiogenesis.  $V_e$  values in HCC were lower, indicative of higher cellularity and decreased sinusoidal spaces. According to the study, combining these DCE-MRI factors could improve the differentiation accuracy between HCC and HCA.

The unique DCE-MRI signatures observed result from the differences in vascularity, permeability, and cellular composition between these two types of hepatic lesions. However, it's important to note that while these studies provide valuable insights, further research, and validation are necessary to establish standardized criteria for using these parameters in clinical practice [25].

However, several limitations warrant consideration. The sample size in our study was relatively modest, and further investigations with larger cohorts are needed to validate our findings and establish more robust diagnostic thresholds. Additionally, the date of sampling for our study

occurred between 2021 and 2022, and this was the most challenging time because of the coronavirus pandemic, the fear of cancer patients visiting hospitals due to their weakened immune systems, and their concern about contracting the Coronavirus, and other factors. In the end, the occurrence of some interruptions in the work of the MRI machine due to maintenance or technical malfunctions.

In conclusion, Our study shows that DCE-MRI and ADC quantification are valuable methods for distinguishing HCC from HCA. Combining functional information from DCE-MRI and microstructural data from ADC studies makes a complete knowledge of hepatic lesions possible. Integrating these advanced imaging techniques holds promise for enhancing diagnostic accuracy and ultimately improving patient outcomes in managing hepatocellular liver tumors.

### Author Contribution Statement

Hayder Suhail NajmAlareer and Ayoob Dinar Abdullah designed the conception of the study; Hayder Jasim Taher conducted the collection and assembly, of data and data analysis and interpretation; Hayder Suhail NajmAlareer and Ayoob Dinar Abdullah performed administrative support and provision of study materials or patients. All authors contributed to the drafted manuscript, revised it critically, and approved the final version.

### Acknowledgements

The authors would like to thank all who supported this survey.

#### Funding statement

This study received no funding support or grants.

#### Conflict of interest

The authors declare no conflicts of interest.

#### Ethical statement

This study was approved by the ethical committee of the Tehran University of Medical Sciences (Ethic code: IR.TUMS.SPH.REC.1398.227). All patients provided informed consent before participation in the study.

#### Availability of data

The authors confirm that the data supporting the findings of this study are available within the article

### References

1. Klompenhouwer AJ, de Man RA, Dioguardi Burgio M, Vilgrain V, Zucman-Rossi J, Ijzermans JNM. New insights in the management of hepatocellular adenoma. *Liver Int.* 2020;40(7):1529-37. <https://doi.org/10.1111/liv.14547>.
2. Bale R, Schullian P, Eberle G, Putzer D, Zoller H, Schneeberger S, et al. Stereotactic radiofrequency ablation of hepatocellular carcinoma: A histopathological study in explanted livers. *Hepatology.* 2019;70(3):840-50. <https://doi.org/10.1002/hep.30406>.
3. Wu H, Wang MD, Liang L, Xing H, Zhang CW, Shen F, et al. Nanotechnology for hepatocellular carcinoma: From surveillance, diagnosis to management. *Small.* 2021;17(6):e2005236. <https://doi.org/10.1002/sml.202005236>.
4. Preuss K, Thach N, Liang X, Baine M, Chen J, Zhang C, et al. Using quantitative imaging for personalized medicine in pancreatic cancer: A review of radiomics and deep learning applications. *Cancers (Basel).* 2022;14(7). <https://doi.org/10.3390/cancers14071654>.
5. Abramson RG, Arlinghaus LR, Dula AN, Quarles CC, Stokes AM, Weis JA, et al. Mr imaging biomarkers in oncology clinical trials. *Magn Reson Imaging Clin N Am.* 2016;24(1):11-29. <https://doi.org/10.1016/j.mric.2015.08.002>.
6. Cuenod CA, Balvay D. Perfusion and vascular permeability: Basic concepts and measurement in dce-ct and dce-mri. *Diagn Interv Imaging.* 2013;94(12):1187-204. <https://doi.org/10.1016/j.diii.2013.10.010>.
7. Roytman M, Kim S, Glynn S, Thomas C, Lin E, Feltus W, et al. Pet/mr imaging of somatostatin receptor expression and tumor vascularity in meningioma: Implications for pathophysiology and tumor outcomes. *Front Oncol.* 2021;11:820287. <https://doi.org/10.3389/fonc.2021.820287>.
8. Kim YS, Kim M, Choi SH, You SH, Yoo RE, Kang KM, et al. Altered vascular permeability in migraine-associated brain regions: Evaluation with dynamic contrast-enhanced mri. *Radiology.* 2019;292(3):713-20. <https://doi.org/10.1148/radiol.2019182566>.
9. Ng SH, Liao CT, Lin CY, Chan SC, Lin YC, Yen TC, et al. Dynamic contrast-enhanced mri, diffusion-weighted mri and (18)f-fdg pet/ct for the prediction of survival in oropharyngeal or hypopharyngeal squamous cell carcinoma treated with chemoradiation. *Eur Radiol.* 2016;26(11):4162-72. <https://doi.org/10.1007/s00330-016-4276-8>.
10. Walker-Samuel S, Leach MO, Collins DJ. Evaluation of response to treatment using dce-mri: The relationship between initial area under the gadolinium curve (iaugc) and quantitative pharmacokinetic analysis. *Phys Med Biol.* 2006;51(14):3593-602. <https://doi.org/10.1088/0031-9155/51/14/021>.
11. Meyers N, Jadoul A, Bernard C, Delwaide J, Lamproye A, Detry O, et al. Inter-observer variability of (90)y pet/ct dosimetry in hepatocellular carcinoma after glass microspheres transarterial radioembolization. *EJNMMI Phys.* 2020;7(1):29. <https://doi.org/10.1186/s40658-020-00302-1>.
12. Lewin M, Fartoux L, Vignaud A, Arrivé L, Menu Y, Rosmorduc O. The diffusion-weighted imaging perfusion fraction f is a potential marker of sorafenib treatment in advanced hepatocellular carcinoma: A pilot study. *Eur Radiol.* 2011;21(2):281-90. <https://doi.org/10.1007/s00330-010-1914-4>.
13. Priyanka C, Rangasami R, Andrew C, Natarajan P. Establishing and comparing the normal apparent diffusion... establishing and comparing the normal apparent diffusion coefficient values of fetal organs and placenta using 1.5 tesla and 3.0 t mri at various gestational age. 2023. <https://doi.org/10.4314/ejhs.v33i4.8>.
14. García-Figueiras R, Padhani AR, Beer AJ, Baleato-González S, Vilanova JC, Luna A, et al. Imaging of tumor angiogenesis for radiologists--part 1: Biological and technical basis. *Curr Probl Diagn Radiol.* 2015;44(5):407-24. <https://doi.org/10.1067/j.cpradiol.2015.02.010>.
15. Zheng R, Wang Q, Lv S, Li C, Wang C, Chen W, et al. Automatic liver tumor segmentation on dynamic contrast enhanced mri using 4d information: Deep learning model based on 3d convolution and convolutional lstm. *IEEE Trans*

- Med Imaging. 2022;41(10):2965-76. <https://doi.org/10.1109/tmi.2022.3175461>.
16. Zhou Y, Zhou G, Zhang J, Xu C, Zhu F, Xu P. Dce-mri based radiomics nomogram for preoperatively differentiating combined hepatocellular-cholangiocarcinoma from mass-forming intrahepatic cholangiocarcinoma. *Eur Radiol*. 2022;32(7):5004-15. <https://doi.org/10.1007/s00330-022-08548-2>.
  17. Ludwig JM, Camacho JC, Kokabi N, Xing M, Kim HS. The role of diffusion-weighted imaging (dwi) in locoregional therapy outcome prediction and response assessment for hepatocellular carcinoma (hcc): The new era of functional imaging biomarkers. *Diagnostics (Basel)*. 2015;5(4):546-63. <https://doi.org/10.3390/diagnostics5040546>.
  18. Garcovich M, Faccia M, Meloni F, Bertolini E, de Sio I, Calabria G, et al. Contrast-enhanced ultrasound patterns of hepatocellular adenoma: An italian multicenter experience. *J Ultrasound*. 2019;22(2):157-65. <https://doi.org/10.1007/s40477-018-0322-5>.
  19. Abdullah AD, Amanpour-Gharaci B, Nassiri Toosi M, Delazar S, Saligheh Rad H, Arian A. Comparing texture analysis of apparent diffusion coefficient mri in hepatocellular adenoma and hepatocellular carcinoma. *Cureus*. 2024;16(1):e51443. <https://doi.org/10.7759/cureus.51443>.
  20. Lee Y, Jee W-H, Whang Y, Jung CK, Chung Y-G, Lee S-Y. Benign versus malignant soft-tissue tumors: Differentiation with 3t magnetic resonance image textural analysis including diffusion-weighted imaging. *Investigative Magnetic Resonance Imaging*. 2021;25:118. <https://doi.org/10.13104/imri.2021.25.2.118>.
  21. Zhang Y, Yang C, Sheng R, Dai Y, Zeng M. Preoperatively identify the microvascular invasion of hepatocellular carcinoma with the restricted spectrum imaging. *Acad Radiol*. 2023;30 Suppl 1:S30-s9. <https://doi.org/10.1016/j.acra.2023.06.010>.
  22. Aronhime S, Calcagno C, Jajamovich GH, Dyvorne HA, Robson P, Dieterich D, et al. Dce-mri of the liver: Effect of linear and nonlinear conversions on hepatic perfusion quantification and reproducibility. *J Magn Reson Imaging*. 2014;40(1):90-8. <https://doi.org/10.1002/jmri.24341>.
  23. Motosugi U, Ichikawa T, Sou H, Sano K, Tominaga L, Muhi A, et al. Distinguishing hypervascular pseudolesions of the liver from hypervascular hepatocellular carcinomas with gadoteric acid-enhanced mr imaging. *Radiology*. 2010;256(1):151-8. <https://doi.org/10.1148/radiol.10091885>.
  24. Kwon HJ, Byun JH, Kim JY, Hong GS, Won HJ, Shin YM, et al. Differentiation of small ( $\leq 2$  cm) hepatocellular carcinomas from small benign nodules in cirrhotic liver on gadoteric acid-enhanced and diffusion-weighted magnetic resonance images. *Abdom Imaging*. 2015;40(1):64-75. <https://doi.org/10.1007/s00261-014-0188-8>.
  25. Li J, Xue F, Xu X, Wang Q, Zhang X. Dynamic contrast-enhanced mri differentiates hepatocellular carcinoma from hepatic metastasis of rectal cancer by extracting pharmacokinetic parameters and radiomic features. *Exp Ther Med*. 2020;20(4):3643-52. <https://doi.org/10.3892/etm.2020.9115>.



This work is licensed under a Creative Commons Attribution-Non Commercial 4.0 International License.